Stem Cell Research 61 (2022) 102773

Contents lists available at ScienceDirect

Stem Cell Research

journal homepage: www.elsevier.com/locate/scr

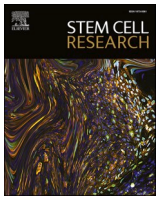

Lab Resource: Multiple Cell Lines

Generation of two human iPSC lines, HMGUi003-A and MRIi028-A, carrying pathogenic biallelic variants in the *PPCS* gene

Arcangela Iuso [a,b,*], Fangfang Zhang [c,d], Ejona Rusha [e], Birgit Campbell [c,d], Tatjana Dorn [c,d], Enrica Zanuttigh [a], Dorothea Haas [f], Yair Anikster [g], Gabriele Lederer [b], Anna Pertek [e], Polyxeni Nteli [e], Karl-Ludwig Laugwitz [c,d], Alessandra Moretti [c,d,*]

[a] *Institute of Neurogenomics, Helmholtz Zentrum München, Munich, Germany*
[b] *Institute of Human Genetics, Technical University of Munich, School of Medicine, Munich, Germany*
[c] *First Department of Medicine, Cardiology, Klinikum Rechts der Isar, Technical University of Munich, School of Medicine & Health, Munich, Germany*
[d] *DZHK (German Centre for Cardiovascular Research), partner site Munich Heart Alliance, Munich, Germany*
[e] *iPSC Core Facility, Helmholtz Zentrum München, Munich, Germany*
[f] *Department of Neuropediatrics and Pediatric Metabolic Medicine, Center for Child and Adolescent Medicine, University Hospital Heidelberg, Heidelberg, Germany*
[g] *Edmond and Lily Safra Children's Hospital, Metabolic Disease Unit, Sackler School of Medicine, Tel Aviv University, Israel and Sheba Medical Center, Tel-Hashomer, Israel*

A B S T R A C T

Phosphopantothenoylcysteine synthetase (PPCS) catalyzes the second step of the *de novo* coenzyme A (CoA) synthesis starting from pantothenate. Mutations in *PPCS* cause autosomal-recessive dilated cardiomyopathy, often fatal, without apparent neurodegeneration, whereas pathogenic variants in *PANK2* and *COASY*, two other genes involved in the CoA synthesis, cause Neurodegeneration with Brain Iron Accumulation (NBIA). PPCS-deficiency is a relatively new disease with unclear pathogenesis and no targeted therapy. Here, we report the generation of induced pluripotent stem cells from fibroblasts of two PPCS-deficient patients. These cellular models could represent a platform for pathophysiological studies and testing of therapeutic compounds for PPCS-deficiency.

1. Resource table

Unique stem cell lines identifier	HMGUi003-A (https://hpscreg.eu/cell-line/HMGUi003-A); MRIi028-A (https://hpscreg.eu/cell-line/MRIi028-A)
Alternative name(s) of stem cell lines	95595 or PPCS-Cl2 (HMGUi003-A); PPC-4 (MRIi028-A)
Institution	Helmholtz Zentrum MünchenKlinikum rechts der Isar (MRI)
Contact information of distributor	Arcangela Iuso, arcangela.iuso@helmholtz-muenchen.de Alessandra Moretti, amoretti@mytum.de
Type of cell lines	iPSCs
Origin	Human
Additional origin info required	HMGUi003-A: female MRIi028-A: male
Cell Source	Skin fibroblasts
Clonality	Clonal
Associated disease	PPCS-deficiency
Gene/locus	HMGUi003-A, NM_024664.4: c.[538G > C]; [320_334del], p.[Ala180Pro]; [Pro107_Ala111del] MRIi028-A, NM_024664.4: c.[698 A > T]; [698 A > T], p.[Glu233Val]; [Glu233Val]
Date archived/stock date	N/A
Cell line repository/bank	https://hpscreg.eu/cell-line/HMGUi003-A https://hpscreg.eu/cell-line/MRIi028-A
Ethical approval	Ethikkommission der Technischen Universität München Approval no. 2109/08

2. Resource utility

Mutations in phosphopantothenoylcysteine synthetase (*PPCS*) lead to autosomal-recessive dilated cardiomyopathy (Iuso et al., 2018). PPCS-deficiency is a rare disorder, with unclear pathogenesis and no therapy. iPSCs from PPCS-deficient patients could provide a platform for disease-relevant models, pathophysiological studies, and testing of

* Corresponding authors at: Institute of Neurogenomics, Helmholtz Zentrum München, Munich, Germany (A. Iuso). First Department of Medicine, Cardiology, Klinikum Rechts der Isar, Technical University of Munich, School of Medicine & Health, Munich, Germany (A. Moretti).
E-mail addresses: arcangela.iuso@helmholtz-muenchen.de (A. Iuso), amoretti@mytum.de (A. Moretti).

https://doi.org/10.1016/j.scr.2022.102773
Received 22 February 2022; Accepted 29 March 2022
Available online 31 March 2022

therapeutic compounds.

3. Resource details

Line HMGUi003-A: Skin fibroblasts from a female patient (Table 1), carrying biallelic heterozygous mutations in the *PPCS* gene (Fig. 1A), were used to generate iPSCs by the vector-free reprogramming system using mRNA for *SOX2*, *KLF4*, *OCT4*, *LIN28*, *NANOG*, and *c-MYC* (Fig. S1A).

Line MRIi028: Skin fibroblasts from a male patient (Table 1), carrying homozygous mutations in the *PPCS* gene (Fig. 1), were used to generate iPSCs by the non-integrating Sendai virus-mediated introduction of OCT3/4, SOX2, c-MYC, and KLF4 (Fig. S1B). We verified iPSCs for loss of Sendai virus expression. The HMGUi003-A line was used as a negative control (Fig. 1B).

Both iPSC lines exhibited typical stem cell morphology, were positive for alkaline phosphatase activity (Fig. 1C), and expressed pluripotency markers, as assessed by immunocytochemistry analysis for NANOG and OCT3/4 (Fig. 1D) and quantitative real-time PCR (qRT-PCR) for *OCT3/4*, *SOX2*, *REX1*, *NANOG*, and *TDGF-1* (Fig. 1E). SOX2 and LIN28A were additionally validated by immunocytochemistry for the HMGUi003-A line (Fig S1C). The differentiation potential of the MRIi028-A and HMGUi003-A lines was demonstrated by the spontaneous *in vitro* differentiation of the iPSCs towards embryoid bodies (EBs), composed of cells from all three germ layers. qRT-PCR analysis revealed expression of markers specific for endoderm (*PDX1*, *SOX7,* and *AFP*), mesoderm (*CD31*, *DES*, *ACTA2*, *SCL,* and *MYL2*), and ectoderm (*CDH5*, *KRT14*, *NCAM1*, *TH,* and *GABRR2*) (Fig. 1F). The HMGUi003-A line was additionally subjected to direct trilineage differentiation and showed expression of *SOX17*, *CXCR4*, *FOXA2* (endoderm), *MESP1*, *T*, *MIXL1* (mesoderm), *PAX6*, and *CDH2* (ectoderm), (Fig. S1D). Both iPSC lines displayed normal karyotype, as determined by G-banding (Table 2 and Fig. 1G). Luminometric tests confirmed the absence of mycoplasma contamination in both lines (Fig. S1E).

4. Materials and methods

4.1. Cell line generation and culturing

HMGUi003-A and MRIi028-A lines were generated from skin fibroblasts using NM-RNA (Reprocell, #00–0076) and the CytoTune-iPS 2.0 Sendai Reprogramming (Thermo Fisher, #A16517) kits, respectively. Fibroblasts were grown in DMEM (Thermo Fisher, #11965092) supplemented with 10% Fetal Bovine Serum (FBS, Thermo Fisher, #16141079), 2 mM L-Glutamine (Thermo Fisher, #25030–081), 1x MEM Non-Essential Amino Acids Solution (Thermo Fisher, #11140050) and 0.055 mM β-mercaptoethanol (Thermo Fisher, #21985023) at 37 °C, 5% CO_2.

iPSCs were cultured as single cells on Geltrex-coated (Thermo Fisher, #A1413302) plates (Falcon, 353,001 and 353004) in Essential 8 medium (E8, Thermo Fisher, #A1517001) containing 0.5% Penicillin/Streptomycin (Thermo Fisher, #15140–122) at 37 °C, 5% CO_2. Medium was changed daily. Cells were passaged at a ratio of 1:14 every 4–5 days using 0.5 mM EDTA (Thermo Fisher, AM9260G). After passaging, the medium was supplemented with 10 μM Thiazovivin (Sigma, SML1045) for 24 h.

4.2. Embryonic body (EB) formation and direct trilineage differentiation

Spontaneous EB differentiation was performed as previously described (Moretti et al., 2010). On day 21, EBs were collected for gene expression analysis. Direct trilineage differentiation was performed as previously reported (Borchin et al., 2013; Ori et al., 2021; Shi et al., 2012). Gene expression was tested on day 5 of differentiation.

4.3. Immunocytochemistry analysis

Cells were fixed with 4% paraformaldehyde (PFA, Sigma, #158127) for 10 min at room temperature (RT), washed twice with DPBS and then blocked and permeabilized with DPBS (Thermo Fisher, #14190144) containing 10% FBS and 0.1% Triton X-100 (Sigma, #X100) for 1 h at

Table 1
Characterization and validation.

Classification	Test	Result	Data
Morphology	Photography brightfield	Visual record of the lines: normal	Fig. 1C
Phenotype	Alkaline phosphatase staining	Staining resulted positive	Fig. 1C
	Immunocytochemistry	Staining of pluripotency markers: NANOG, OCT3/4 (SOX2, LIN28 additionally for the HMGUi003-A line)	Fig. 1D (Fig. S1C)
	qRT-PCR	Expression of pluripotency markers *OCT3/4*, *SOX2*, *REX1*, *NANOG*, *TDGF-1*.	Fig. 1E
	RT-PCR	Loss of Sendai virus for the MRIi028-A line	Fig. 1B
Genotype	Karyotype (G-banding) and resolution	HMGUi003-A line: 46XX, resolution 450-550. MRIi028-A line: 46XY, resolution 500-600.	Fig. 1G
Identity	Microsatellite PCR (mPCR) OR	N/A	
	STR analysis	The 16 sites tested, all matching	Data available with the authors
Mutation analysis	Sequencing	HMGUi003-A NM_024664.4: c. [538G>C]; [320_334del], p. [Ala180Pro]; [Pro107_Ala111del]. MRIi028-A NM_024664.4: c. [698 A>T]; [698 A>T], p. [Glu233Val]; [Glu233Val].	Fig. 1A
	Southern Blot OR WGS	N/A	
Microbiology and virology	Mycoplasma	Mycoplasma testing by luminescence: Negative	Fig. S1E
Differentiation potential	Embryoid body formation (Directed trilineage differentiation additionally for the HMGUi003-A line)	Expression of the three germ layers formation: mesoderm, endoderm, ectoderm	Fig. 1F (Fig. S1D)
List of recommended germ layer markers	**Expression of these markers has to be demonstrated at mRNA (RT PCR)**	Endoderm: *PDX1*, *SOX7*, *AFP*, *SOX17* (SOX17, *CXCR4*, *FOXA2* additionally for HMGUi003-A). Mesoderm: *CD31*, *DES*, *ACTA2*, *SCL*, *MYL2*, *CDH5* (*MESP1, T*, *MIXL1* additionally for HMGUi003-A). Ectoderm: *KRT14*, *NCAM1*, *TH*, *GABRR2* (*PAX6*, *CDH2* additionally for HMGUi003-A).	Fig. 1F and Fig. S1D
Donor screening (OPTIONAL)	HIV 1 + 2 Hepatitis B, Hepatitis C	N/A	
Genotype additional info (OPTIONAL)	Blood group genotyping	N/A	
	HLA tissue typing	N/A	

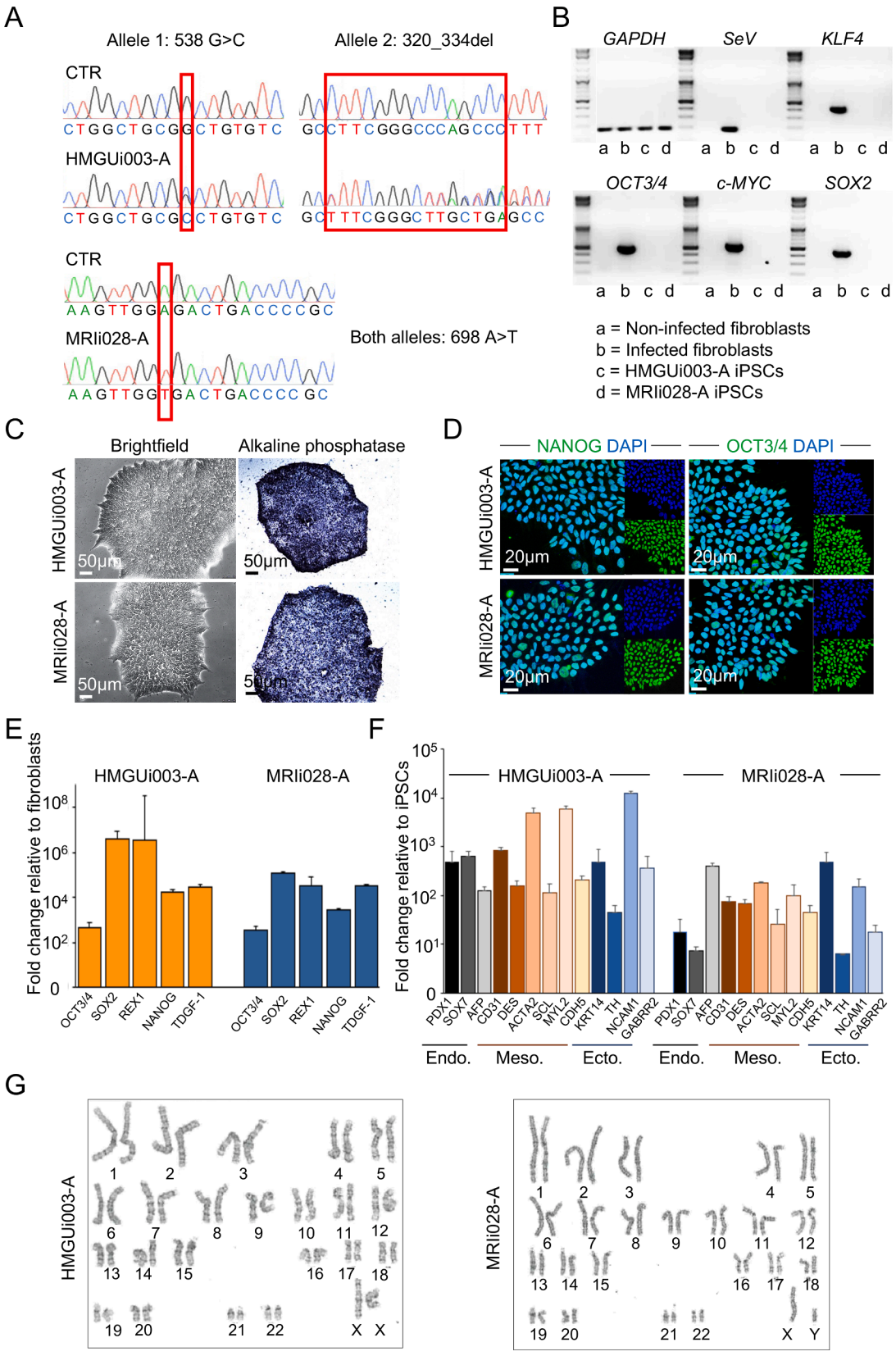

Fig. 1. A) Sanger sequences of the HMGUi003-A and MRIi028-A lines. B) Sendai virus expression by RT-PCR. C) Morphology of iPSC colonies in brightfield and alkaline phosphatase staining. D-E) Expression of master regulators of pluripotent stem cells and associated markers, assessed by immunofluorescence for *NANOG* and *OCT3/4* (D), and qRT-PCR for *OCT3/4*, *SOX2*, *REX1*, *NANOG*, and *TDGF-1* (E). F) Endogenous expression of the three germ layers markers *PDX1*, *SOX7*, *AFP*, *CD31*, *DES*, *ACTA2*, *SCL*, *MYL2*, *CDH5*, *KRT14*, *TH*, *NCAM1*, *GABRR2* by qRT-PCR. G) Karyotyping by G-banding.

Table 2
Reagents details.

	Antibodies used for immunocytochemistry/flow-cytometry			
	Antibody	Dilution	Company Cat #	RRID
Pluripotency markers	Rabbit anti-OCT3/4	0.1806	Abcam Cat #ab19857	RRID: AB_445175
	Rabbit anti-NANOG	0.1806	Abcam Cat #ab21624	RRID: AB_446437
	AF488 mouse anti human TRA-1-81	1:20	BD Pharmingen Cat #560174	RRID: AB_1645380
	Rabbit OCT-4a	0.3194	CST Cat #2840S	RRID:AB_2167691
	Rabbit SOX2	0.1806	CST Cat #2748S	RRID:AB_823640
	Rabbit NANOG	0.1806	CST Cat #4903S	RRID:AB_10559205
	Rabbit LIN28A	0.5972	CST Cat #3978S	RRID:AB_2297060
Secondary antibodies	Goat anti-Rabbit AF488 IgG	0.3889	Thermo Fisher Cat #A-11008	RRID: AB_143165
	Goat anti-Rabbit IgG (H+L) Highly Cross-Adsorbed, AF 488	0.7361	Thermo Fisher Cat #A-11034	RRID:AB_2576217
Nuclear stain	Hoechst 33258	1 μg/ml	Sigma Cat #94403	
	ProLong Glass Antifade Mountant with NucBlue Stain (Hoechst 33342)	N/A	Thermo Fisher Cat #P36985	

	Primers		
	Target	Size of band	Forward/Reverse primer (5′-3′)
RT-PCR Sendai virus genes	*SeV*	181	GGATCACTAGGTGATATCGAGC/ACCAGACAAGAGTTTAAGAGATATGTATC
RT-PCR Sendai virus genes	*OCT3/4 SeV*	149	GGGATGGCGTACTGTGGG/GCACCAGGGGTGACGGTG
RT-PCR Sendai virus genes	*SOX2 SeV*	192	AGCAGACTTCACATGTCCCAG/ACCGGGTTTTCTCCATGCTGT
RT-PCR Sendai virus genes	*c-MYC SeV*	102	CACCAGCAGCGACTCTGA/GATCCAGACTCTGACCTTTTGC
RT-PCR Sendai virus genes	*KLF4 SeV*	134	TCTTCGTGCACCCACTTGGG/CTGCTCAGCACTTCCTCAAG
Sequencing	*PPCS* c.698 A>T	467	GGCCAAGCCACTGTGTTCCC/GCTGTGTGTCGAGACTGAAG
Sequencing	*PPCS* c.538G>C	682	CTGAGGCTCTGAGGAGCTAC/CAAGAAGCTTCATCGACTCC
Sequencing	*PPCS* c.320_334del	634	ATGGCGGAAATGGATCCGG/AGGATCAGCTCCTTCTCAAC
qRT-PCR Pluripotency markers	*OCT3/4*	144	GACAGGGGGAGGGGAGGAGCTAGG/CTTCCCTCCAACCAGTTGCCCCAAAC
qRT-PCR Pluripotency markers	*SOX2*	151	GGGAAATGGGAGGGGTGCAAAAGAGG/TTGCGTGAGTGTGGATGGGATTGGTG
qRT-PCR Pluripotency markers	*NANOG*	116	TGCAAGAACTCTCCAACATCCT/ATTGCTATTCTTCGGCCAGTT
qRT-PCR Pluripotency markers	*REX1*	445	ACCAGCACACTAGGCAAACC/TTCTGTTCACACAGGCTCCA
qRT-PCR Pluripotency markers	*TDGF1*	139	CCCAAGAAGTGTTCCCTGTG/ACGTGCAGACGGTGGTAGTT
qRT-PCR Three germ layers markers	*PDX1*	190	GATGAAGTCTACCAAAGCTCACG/GTTCAACATGACAGCCAGCTC
qRT-PCR Three germ layers markers	*SOX7*	112	TGAACGCCTTCATGGTTTG/AGCGCCTTCCACGACTTT
qRT-PCR Three germ layers markers	*AFP*	101	GTGCCAAGCTCAGGGTGTAG/CAGCCTCAAGTTGTTCCTCTG
qRT-PCR Three germ layers markers	*CD31*	108	ATGCCGTGGAAAGCAGATAC/CTGTTCTTCTCGGAACATGGA
qRT-PCR Three germ layers markers	*MYL2*	138	TACGTTCGGGAAATGCTGAC/TTCTCCGTGGGTGATGATG
qRT-PCR Three germ layers markers	*DES*	115	GTGAAGATGGCCCTGGATGT/TGGTTTCTCGGAAGTTGAGG
qRT-PCR Three germ layers markers	*ACTA2*	112	GTGATCACCATCGGAAATGAA/TCATGATGCTGTTGTAGGTGGT
qRT-PCR Three germ layers markers	*SCL*	98	CCAACAATCGAGTGAAGAGGA/CCGGCTGTTGGTGAAGATAC
qRT-PCR Three germ layers markers	*CDH5*	75	CCTACCAGCCCAAAGTGTGT/TGTCCTTGTCTATTGCGGAGA
qRT-PCR Three germ layers markers	*KRT14*	86	CACCTCTCCTCCTCCCAGTT/ATGACCTTGGTGCGGATTT
qRT-PCR Three germ layers markers	*NCAM1*	136	CAGATGGGAGAGGATGGAAA/CAGACGGGAGCCTGATCTCT
qRT-PCR Three germ layers markers	*TH*	120	TGTACTGGTTCACGGTGGAGT/TCTCAGGCTCCTCAGACAGG
qRT-PCR Three germ layers markers	*GABRR2*	106	CTGTGCCTGCCAGAGTTTCA/ACGGCCTTGACGTAGGAGA
qRT-PCR/RT-PCR House-keeping genes	*GAPDH*	167	TCCTCTGACTTCAACAGCGA/GGGTCTTACTCCTTGGAGGC
qRT-PCR Three germ layers markers (Fig. S1D)	*SOX17*	61	GGCGCAGCAGAATCCAGA/CCACGACTTGCCCAGCAT
qRT-PCR Three germ layers markers (Fig. S1D)	*CXCR4*	79	CACCGCATCTGGAGAACCA/GCCCATTTCCTCGGTGTAGTT
qRT-PCR Three germ layers markers (Fig. S1D)	*FOXA2*	89	GGGAGCGGTGAAGATGGA/TCATGTTGCTCACGGAGGAGTA
qRT-PCR Three germ layers markers (Fig. S1D)	*MESP1*	102	CTGCCTGAGGAGCCCAAGT/GCAGTCTGCCAAGGAACCA
qRT-PCR Three germ layers markers (Fig. S1D)	*T*	101	CAACCTCACTGACGGTGAAAAA/ACAAATTCTGGTGTGCCAAAGTT
qRT-PCR Three germ layers markers (Fig. S1D)	*MIXL1*	58	CCGAGTCCAGGATCCAGGTA/CTCTGACGCCGAGACTTGG
qRT-PCR Three germ layers markers (Fig. S1D)	*PAX6*	95	GCGGAGTTATGATACCTACACC/GAAATGAGTCCTGTTGAAGTGG
qRT-PCR Three germ layers markers (Fig. S1D)	*CDH2*	51	CCCACACCCTGGAGACATTG/GCCGCTTTAAGGCCCTCA
qRT-PCR House-keeping genes (Fig. S1D)	*GAPDH*	184	GCTCATTTCCTGGTATGACAACG/GAGATTCAGTGTGGTGGGGG

RT followed by incubation with primary antibodies in DPBS with 1% FBS and 0.1% Triton X-100 overnight at 4 °C. After washing, secondary antibodies and 5 μg/ml Hoechst 33258 (Sigma, #94403) were incubated for 1 h at RT. Primary and secondary antibodies are listed in Table 2. Images were acquired with a TCS SP8 confocal laser scanning microscope (Leica Microsystems).

4.4. Quantitative real-time PCR (qRT-PCR) and reverse transcription PCR (RT-PCR)

Total RNA was isolated with the Absolutely Microprep RNA (Agilent, #400805) or the RNeasy Mini (Qiagen, #74106) kits and 1 μg was used to synthesize cDNA with the High-Capacity cDNA Reverse Transcription kit (Applied Biosystems, #4368813). For RT-PCR analysis, 1 μl cDNA was subjected to subsequent PCR using Q5 High-Fidelity DNA Polymerase (BioLabs, #M0491S). qRT-PCR was performed with 1 μl cDNA, Power SYBR Green PCR Master Mix (Applied Biotechnologies, #4367659) and primers listed in Table 2 using a 7500 Fast Real-Time PCR instrument (Applied Biosystems). Gene expression levels were normalized to *GAPDH*.

4.5. Alkaline phosphatase activity detection

Direct alkaline phosphatase activity was analyzed using the NBT/BCIP alkaline phosphatase blue substrate (Roche, #11681451001), according to the manufacturer's instructions.

4.6. Karyotyping

Karyotyping was performed via metaphase preparation and G-banding (≥20 metaphases counted) at the Institute of Human Genetics of the Technical University of Munich.

4.7. Sequencing

Genomic DNA was isolated using DNeasy Blood & Tissue Kit

(Qiagen, # 69504) according to the manufacturer's instructions. The *PPCS* gene was amplified at the three mutations sites by PCR using Herculase II Fusion DNA Polymerase (Fisher Scientific, #NC1683759) and Sanger sequenced (Eurofins MWG Operon) (Primers are listed in Table 2).

4.8. Mycoplasma

Mycoplasma detection was performed with the MycoAlert PLUS Mycoplasma Detection Kit (Lonza, #LT07-703) according to the manufacturer's instructions.

4.9. STR analysis

STR analysis of reprogrammed cell lines was performed by Eurofins MWG Operon.

4.10. Cell lines identity testing

Cell line identity testing was performed using STR analysis and validation of the *PPCS*-specific mutations by Sanger sequencing.

4.11. Abnormal karyotype

N/A.

Declaration of Competing Interest

The authors declare that they have no known competing financial interests or personal relationships that could have appeared to influence the work reported in this paper.

Acknowledgements

This work was supported by grants from: the European Research Council (ERC), (788381 to A.M.); the German Centre for Cardiovascular Research (DZHK), (FKZ 81Z0600601 to A.M. and K-L.L.).

Appendix A. Supplementary data

Supplementary data to this article can be found online at https://doi.org/10.1016/j.scr.2022.102773.

References

Borchin, B., Chen, J., Barberi, T., 2013. Derivation and FACS-mediated purification of PAX3+/PAX7+ skeletal muscle precursors from human pluripotent stem cells. Stem Cell Rep. 1, 620–631. https://doi.org/10.1016/j.stemcr.2013.10.007.

Iuso, A., Wiersma, M., Schüller, H.-J., Pode-Shakked, B., Marek-Yagel, D., Grigat, M., Schwarzmayr, T., Berutti, R., Alhaddad, B., Kanon, B., Grzeschik, N.A., Okun, J.G., Perles, Z., Salem, Y., Barel, O., Vardi, A., Rubinshtein, M., Tirosh, T., Dubnov-Raz, G., Messias, A.C., Terrile, C., Barshack, I., Volkov, A., Avivi, C., Eyal, E., Mastantuono, E., Kumbar, M., Abudi, S., Braunisch, M., Strom, T.M., Meitinger, T., Hoffmann, G.F., Prokisch, H., Haack, T.B., Brundel, B.J.J.M., Haas, D., Sibon, O.C. M., Anikster, Y., 2018. Mutations in PPCS, encoding phosphopantothenoylcysteine synthetase, cause autosomal-recessive dilated cardiomyopathy. Am. J. Hum. Genet. 102, 1018–1030. https://doi.org/10.1016/j.ajhg.2018.03.022.

Moretti, A., Bellin, M., Welling, A., Jung, C.B., Lam, J.T., Bott-Flügel, L., Dorn, T., Goedel, A., Höhnke, C., Hofmann, F., Seyfarth, M., Sinnecker, D., Schömig, A., Laugwitz, K.-L., 2010. Patient-specific induced pluripotent stem-cell models for long-QT syndrome. N. Engl. J. Med. 363, 1397–1409. https://doi.org/10.1056/NEJMoa0908679.

Ori, C., Ansari, M., Angelidis, I., Theis, F.J., Schiller, H.B., Drukker, M., 2021. Single cell trajectory analysis of human pluripotent stem cells differentiating towards lung and hepatocyte progenitors (preprint). Developmental Biol. https://doi.org/10.1101/2021.02.23.432413.

Shi, Y., Kirwan, P., Livesey, F.J., 2012. Directed differentiation of human pluripotent stem cells to cerebral cortex neurons and neural networks. Nat. Protoc. 7, 1836–1846. https://doi.org/10.1038/nprot.2012.116.